

## Numerical Modelling of Wind Patterns around a Solar Parabolic Trough Collector

Mahesh Dundage<sup>1</sup>, R. O. Bhagwat<sup>2</sup>, Suhas Chavan<sup>3</sup>

<sup>1,2</sup>Department of Mechanical Engineering, VJTI, Mumbai, India

<sup>3</sup>Solar-CoE, Thermax Limited, Pune, India

**ABSTRACT:** Solar based energy systems are now becoming very popular nowadays. Solar parabolic trough collectors are widely used for solar heating and solar thermal power plant. One aspect that is very important is the exact determination of drag force acting on the systems. To calculate drag force, drag coefficient, which is always associated with a particular area, is required. This drag coefficient can be determined by experimentally or by numerical simulation.

This study reports on numerical predictions of drag coefficient, velocity and pressure fields in steady flow around a solar parabolic trough collector. Also the wind load acting on the collector is determined for each position of trough. In this paper drag coefficients are evaluated for different pitch angles ( $0^\circ$  to  $180^\circ$ ) of parabolic trough using the computational fluid dynamics (CFD) software for wind velocity of 12m/s. Also for  $0^\circ$  pitch angle, drag coefficient is calculated varying wind velocity from 8m/s to 18m/s. It is found that maximum drag coefficient is 1.71 at  $0^\circ$  pitch angle and drag coefficient remains constant for wind velocity range 8m/s to 18m/s. The present study has established that commercially available software like can provide a reasonable good solution of complicated flow structures.

**Keywords:** CFD, Drag coefficient, Drag force, Numerical simulation, solar parabolic trough collector

### I. INTRODUCTION

It is an accepted fact that solar energy, which has attracted more attention during the recent years, is a form of sustainable energy. Sunlight can be used directly for heating and lighting residential and commercial buildings. The heat of sun can be harnessed for hot water heating, solar cooling, and other commercial and industrial uses. Today a great variety of solar technologies for electricity generation are available and among many, the application of parabolic collectors in large sizes is employed in many systems. Parabolic trough technology is currently the most proven solar thermal electric technology in the world. This is primarily due to nine large commercial scale solar power plants installed in USA. Large fields of parabolic trough collectors supply the thermal energy needed to produce steam for a Rankine steam turbine/generator cycle. Parabolic collectors have been also used or are under construction for commercial power plants in many countries such as Egypt, Greece, India, Mexico and Spain.

The major components of the parabolic collector are the receiver tube, the reflector, tracking system, collector structure, etc. The receiver is the element of the system, where solar radiation is absorbed and converted the radiated energy to thermal energy. It includes the absorber, its associated glass covers, and insulation. Solar parabolic trough collectors are arranged in modules so as to get required temperature rise and mass flow rate of the working fluid. For such solar collector, its ability to track the sun with respect to time very accurately is important. Any small off tracking as well as the collector structure stability will be affected by wind blowing from the regions, where the wind velocity is high.

Earlier wind flow studies around parabolic shape structure such as trough collectors were rare. But, today, with the increased interest in the solar energy, study of wind flow around parabolic trough is increasing. Wind load acting on an object can be determined using standard codes or by experimental graphs available. But these codes and graphs are for standard objects like sphere, rectangular plate, cylinder etc. Other shapes of objects need wind tunnel test or field test for wind load estimation. These tests are expensive and more importantly time consuming. Numerical modelling of flow can provide reasonably good values of drag coefficient and wind load estimates.

Farid C. Christo studied wind pattern around the full scale paraboloidal solar dish. In this paper velocity and pressure field around the dish were predicted using numerical modelling. The SST  $k-\omega$  turbulence model, and a second-order upwind discretisation schemes are used for all equations. Study was done for different pitching angles ( $0^\circ$  to  $180^\circ$ ) and for different velocities. Aerodynamic coefficients for different positions were calculated. Analysis was done for both steady and unsteady flows around the dish and it was concluded that coefficients for steady and unsteady flows are same. It was found that aerodynamic coefficients were independent on wind velocity. The effects of installing windbreaks on aerodynamic forces were studied. Overall the results of numerical modelling were satisfactory. N. Naeni et al. studied wind flow around a parabolic trough which is being used in solar thermal power plant. Computation is carried out for wind velocity ranging from 5 to 15 m/s and for different pitching angles ( $90^\circ$ ,  $60^\circ$ ,  $30^\circ$ ,  $0^\circ$ ,  $-90^\circ$ ,  $-60^\circ$ ,  $-30^\circ$ ). Simulation was done in two dimensions and using RNG  $k-\epsilon$  turbulent model. Analysis included the effect of velocity boundary layer in the calculation. Girma T. Bitsuamlak et al. evaluated wind loads on solar panel modules using CFD method. In the analysis, position of the panel was fixed and angle of attack was varied. Calculations were done for stand-alone and arrayed panel type structure. Numerical results were validated with the experimental results. Yazan Taamneh carried out computational fluid dynamics (CFD) simulations for incompressible fluid flow around ellipsoid in laminar steady axisymmetric regime. Analysis was carried out for major to minor axis ratio ranged over 0.5 to 2. Flow around ellipsoid was visualized for different axis ratio. The simulation results are presented in terms of skin friction coefficient, separation angles and drag coefficient. Same simulation procedure was used for flow around sphere and simulation results were validated with experimental results. It was concluded

that commercially available software like FLUENT can provide a reasonable good solution of complicated flow structures including flow with separation. Shaharin A Sulaiman studied air flow over a two-dimensional cylindrical object using ANSYS CFD Flotran to obtain the surface pressure distribution, from which drag and lift were calculated using integral equations of pressure over finite surface areas. In addition the drag and lift coefficients were also determined. The simulation was repeated for various Reynolds numbers to check the robustness of the method. The CFD simulation results show close agreement with those of the experiment. Georgeta Văsieș et al. carried out the numerical simulations for analysis of wind action on solar panels, located on flat roofs with and without parapets. Analysis was done for wind incident angle of  $45^\circ$  and the distribution of pressure on solar panels installed in a compact field on a flat roof was determined. Bo Gong et al. conducted an experiment on field to determine wind load on parabolic trough and characteristics of wind i.e. wind speed, wind direction and boundary layer formation. The objective of this study was to investigate wind loads and wind characteristics on parabolic trough solar collectors under wind action. The wind loads and wind characteristics on collector were measured using wind pressure transducers and propeller anemometers, respectively. Various test configurations were examined, consisted of 12 phases and every phase corresponds to a pitch angle of the solar collector.

The objectives of the study are; to determine the drag coefficient for a solar parabolic trough collector for different pitch angles; to determine the drag force acting on a solar parabolic trough collector for different pitch angles; to determine the effect of wind velocity on drag coefficient; to observe the velocity and pressure contours around the trough.

## II. MODEL OF PARABOLIC TROUGH

In a solar thermal power plant there is an array of parabolic trough to reach the required high temperature. But for the study, geometry of a single repetitive unit has been considered. Several numerical and experimental studies have been performed to assess the heat transfer aspects of this parabolic trough. However, only a few studies of flow field have been published for parabolic trough.

The parabolic trough has a focal length of 500 mm and a total reflecting surface area (A) of approximately 7.931 m<sup>2</sup>. Its axis of rotation is assumed to be located approximately 1.233 m above ground level. The pitch angle of the parabolic trough is shown in Fig.1.

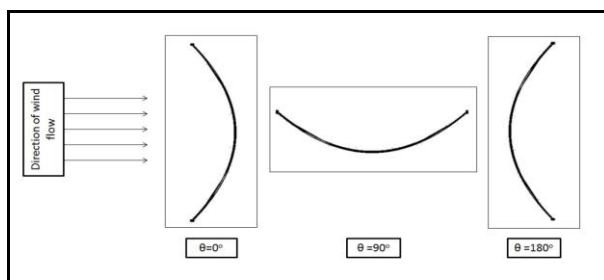


Figure 2: Parabolic trough collector in three positions with respect to wind

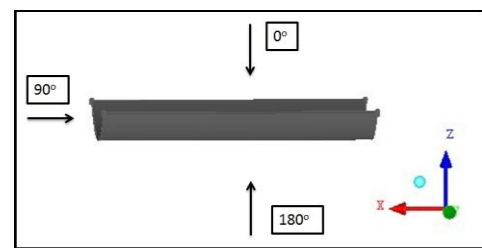


Figure 1: Wind incident angle from  $0^\circ$  to  $180^\circ$  for  $0^\circ$  pitch angle

For pre-processing ICFM CFD was used. All calculations were performed using the ANSYS FLUENT package. A high-quality and fine mesh is constructed over the entire computational domain. The external domain around the parabolic trough extends 1000mm downstream and 500mm in lateral directions, resulting in the parabolic trough occupying less than 0.015% of the volume of the computation domain. This ratio is deemed adequate for modelling external flows with minimal effect of pressure boundaries proximity to the parabolic trough. Although the parabolic trough sits in an atmospheric boundary layer, the calculations assumed a uniform, rather than a boundary-layer, inlet velocity profile. This assumption represents a worst-case scenario for structural loading, hence effectively incorporates a design safety factor.

Steady-state calculations are performed for different pitch angle ( $\theta$ ) and wind speed ( $V$ ) scenarios. The realizable  $k-\epsilon$  turbulence model is used for all equations. Solution convergence is determined by ensuring all residuals of the transport equations drop below a pre-determined threshold and that drag coefficient does no longer vary with iterations.

## III. MODEL VALIDATION

Validation of the numerical model is carried out using data from wind tunnel experiments conducted on a parabolic trough collector. In this experiment, parabolic trough is kept at  $0^\circ$  pitch angle and wind incident angle ( $\alpha$ ) is changed from  $0^\circ$  to  $180^\circ$  i.e. over entire  $180^\circ$  as shown in Fig.2. This reference is used because it provides sufficient information about the trough and the wind-tunnel geometry and flow conditions to generate an accurate numerical model. In the wind tunnel test results, drag coefficient at different wind incident angles for different wind speed were determined.

Numerical modelling was done for these test results. The predicted numerical drag coefficients (Fig.3) found to deviate by 15%, 16%, and 17%, 18%, 18% respectively, from the mean experimental values. Largest drag coefficient and drag force occurs at  $0^\circ$  pitch angle. Overall the predicted drag coefficients are acceptable. This outcome therefore validates the accuracy of the calculations and provides confidence in the numerical model. Extensive experimental work is carried out on flow over the sphere. So the flow over the sphere was modelled numerically so as to check whether the numerical method gives results with minimum error or not. Maximum deviation for flow over sphere was about 18% (Fig.4).

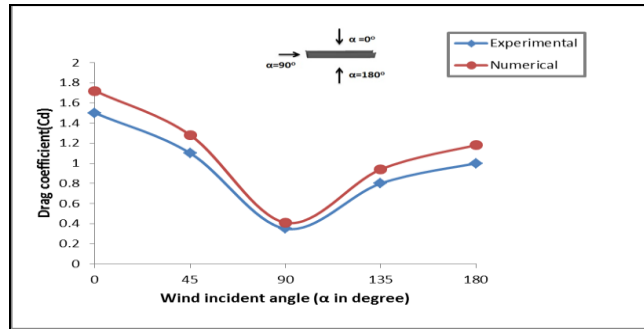


Figure 3: Experimental and numerical drag coefficient against wind incident angle for parabolic trough

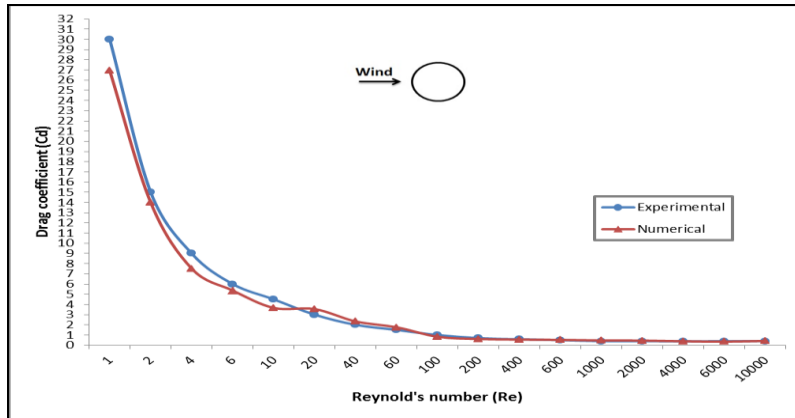


Figure 4: Experimental and numerical drag coefficient against Reynolds's number for sphere

In both the cases, maximum deviation from experimental value is about 18%. Nature of the curve in both the cases was nearly same. This outcome therefore validates the accuracy of the calculations and provides confidence in the numerical model.

#### IV. RESULTS AND DISCUSSIONS

Three-dimensional calculations are performed for the parabolic trough oriented at different pitch angles  $0^\circ$ ,  $30^\circ$ ,  $60^\circ$ ,  $90^\circ$ ,  $120^\circ$ ,  $150^\circ$ , and  $180^\circ$ . For pitch angle  $0^\circ$  calculations are repeated for wind speed 8, 10, 12, 14, 16 and 18 m/s.

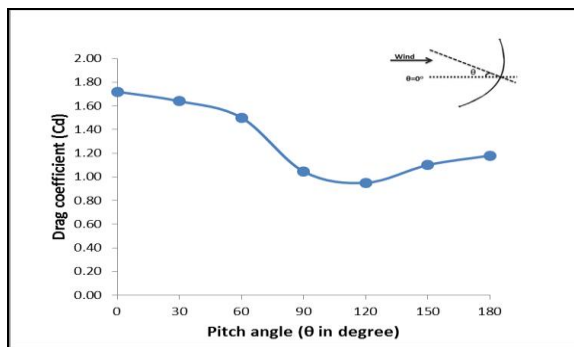


Figure 5: Predicted drag coefficient against pitch angle for parabolic trough

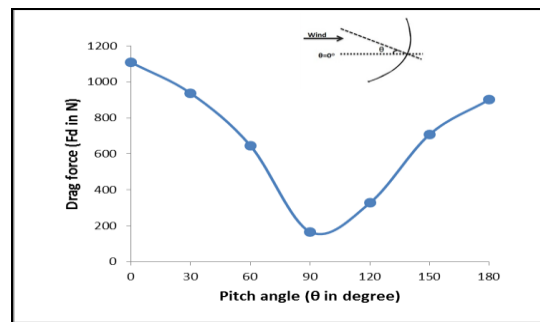


Figure 6: Predicted drag force against pitch angle for parabolic trough

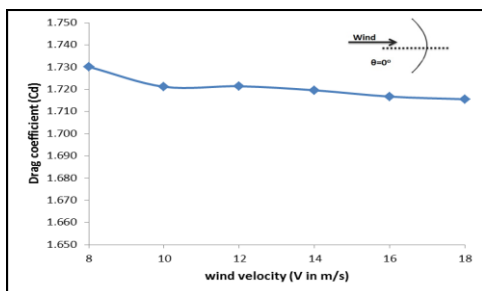


Figure 7: Drag coefficient against wind speed for trough at  $0^\circ$  pitch angle

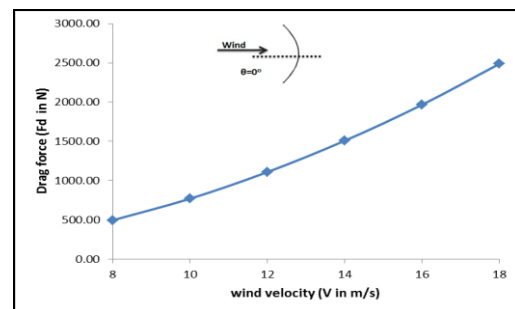


Figure 8: Drag force against wind speed for trough at  $0^\circ$  pitch angle



For the steady-state flow conditions the predicted drag and coefficients (as expected) are independent of wind speeds, (Fig.8) but are strongly influenced by the pitch angle (Fig.6). Maximum drag coefficient occurs at  $0^\circ$  pitch angle and minimum at  $120^\circ$  pitch angle. Though the projected area is minimum at  $90^\circ$  pitch angle, it is not a position of minimum drag coefficient. This is because drag coefficient depends on flow structure around trough and pressure difference caused around the trough. For the given range of velocity drag coefficient is constant. Drag force increases gradually with increase in the wind velocity (Fig.7). Maximum drag force occurs at  $0^\circ$  position which is equal to 1100 N. Drag force decreases with increase in pitch angle up to  $90^\circ$  pitch angle. Again it increases from  $90^\circ$  to  $180^\circ$  pitch angle.

The flow field around the trough is shown in the following figures. For different positions of trough, flow structure around the trough is different. Flow separation has occurred at upper edges of the trough (Fig.11). For  $0^\circ$  and  $180^\circ$  positions two vortices are formed at leeward side of the trough. For other positions single vortex is formed. This is because  $0^\circ$  and  $180^\circ$  positions are symmetrical positions. Single vortex is formed at lower region of the trough for  $30^\circ$  pitch angle.  $60^\circ$  position is slightly streamlined with the flow. No larger vortex appears for this position. But the vortex is visible at  $z=0$  plane as shown in Fig.10. For  $90^\circ$  position single vortex is formed inside the concave region of the trough. For  $120^\circ$  and  $150^\circ$  position single vortex is formed. For  $120^\circ$  position vortex is formed at middle part of the trough and for  $150^\circ$  position vortex is at upper part of trough. Last three positions i.e.  $120^\circ$ ,  $150^\circ$ ,  $180^\circ$  positions are slightly streamlined. Hence the value of the drag coefficient for these positions is less than that of  $0^\circ$ ,  $30^\circ$ ,  $60^\circ$  positions.

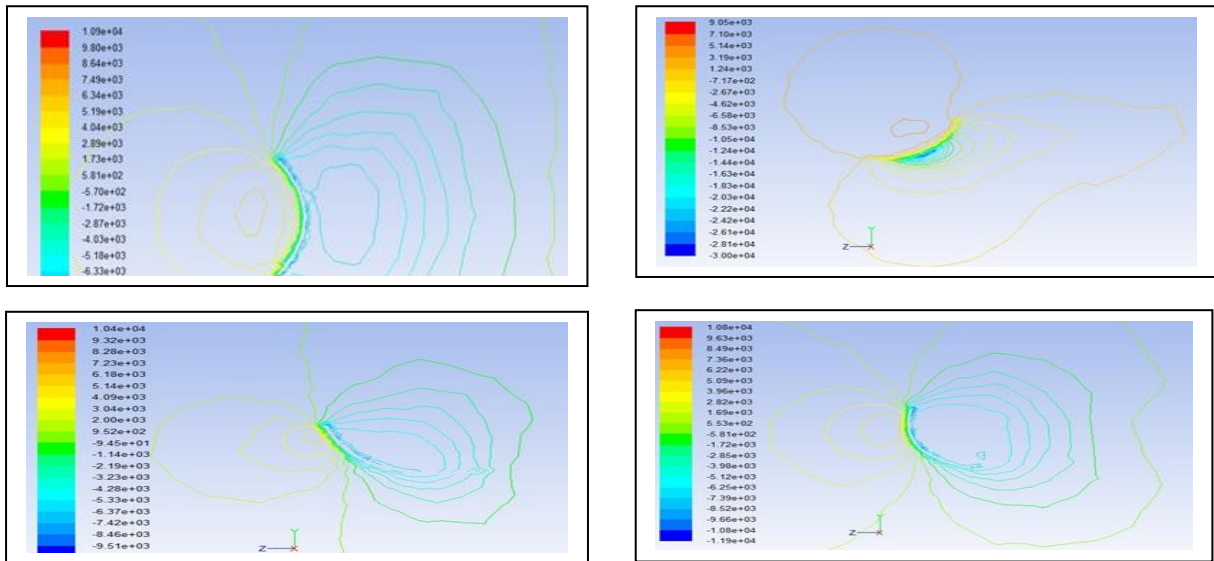
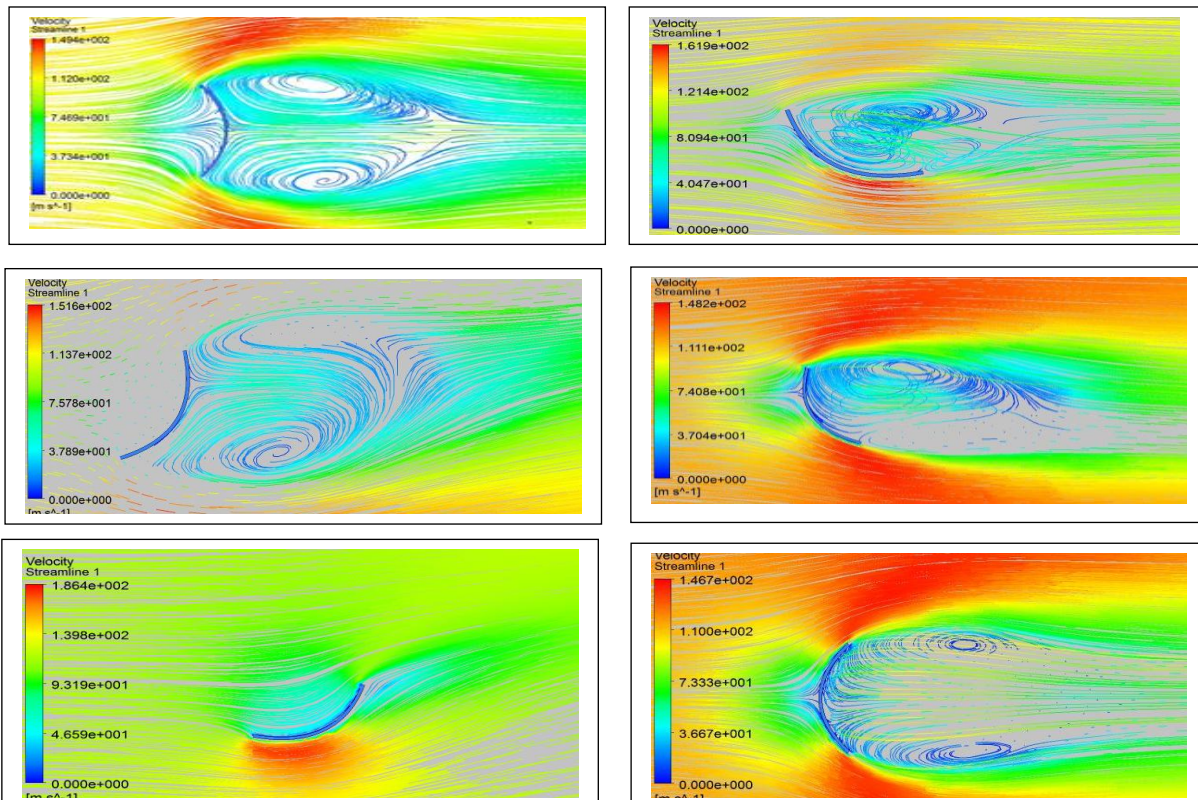


Figure 5: Contours of static pressure for  $0^\circ$ ,  $60^\circ$ ,  $120^\circ$ ,  $150^\circ$



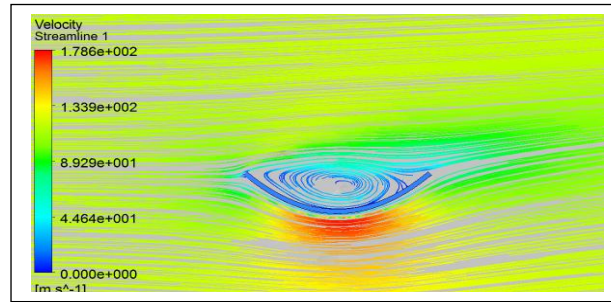


Figure 60: Contours of velocity streamlines for different trough positions

## V. CONCLUSION

This validated numerical study provides a quantitative assessment of velocity and pressure fields around a parabolic trough collector.

- Maximum drag coefficient occurs at  $0^\circ$  pitch angle and its value is 1.72. Minimum drag coefficient occurs at  $120^\circ$  pitch angle and its value is 0.95.
- Maximum drag force is 1100N and minimum drag force is 167N occurs at  $0^\circ$  and  $90^\circ$  pitch angle respectively.
- Various recirculation regions can be found on the leeward and forward sides of the parabolic trough collector when the pitch angle changes with respect to wind direction.
- The resultant force on the collector structure is maximum when wind blows normal to the opening and minimum when the collector is oriented parallel with wind direction.
- The wind force on the collector structure and reflectors increases sharply when the wind speed increases, especially for large collector angles against wind direction.
- The resultant force on the mirrors to pull them from their support is maximum when the convex part of collector is against wind direction.
- Thus, this numerical method gives fairly good results of drag coefficient and flow structure around trough. This method is also useful for other solar concentrators like solar dish for determination of drag coefficient.

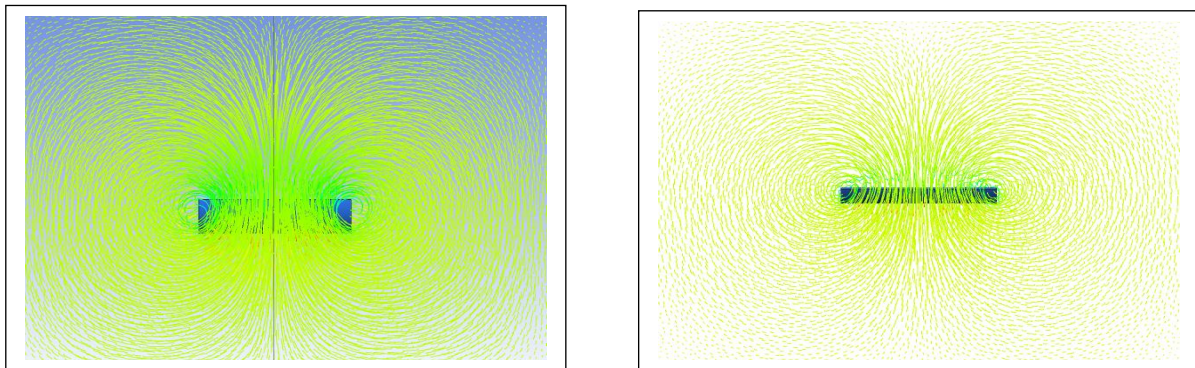


Figure 71: Contours of velocity streamlines for pitch angle of  $60^\circ$  and  $90^\circ$  at a plane  $z=0$

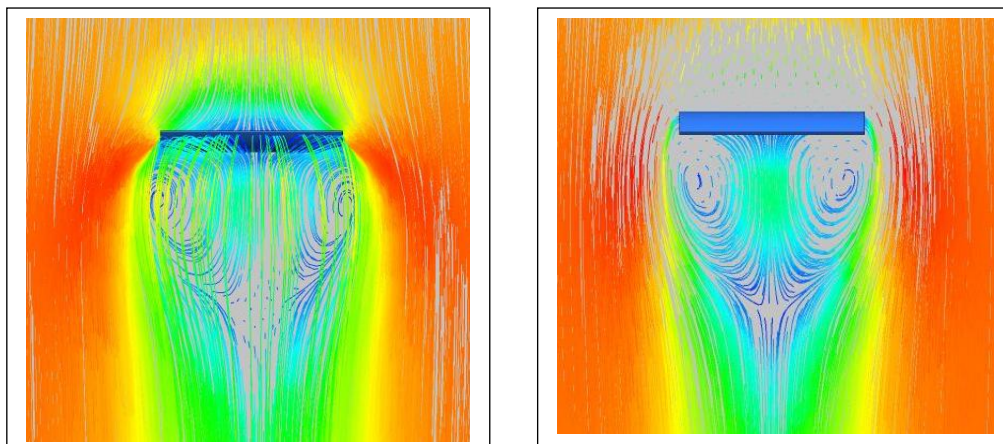


Figure 8: Contours of velocity streamlines for pitch angle of  $0^\circ$  and  $180^\circ$  at a plane  $y=0$



## VI. ACKNOWLEDGEMENTS

The work described in this paper was undertaken in Thermax Limited, Pune. Thanks to Thermax Limited, Pune for giving an opportunity to work on this project. Thanks to Mr. K. V. Deshpande, General Manager and Head- Solar CoE, Thermax Limited, Pune, for his encouragement and support while doing this work.

## REFERENCES

- [1]. Farid C. Christo, Numerical modelling of wind and dust patterns around a full-scale paraboloidal solar dish, *Renewable Energy*, 39, 2011, 356-366.
- [2]. N. Naeeni, M. Yaghoubi, Analysis of wind flow around a parabolic collector (1) fluid flow, *Renewable Energy*, 32, 2006, 1898-1916.
- [3]. Yazan Taamneh, CFD Simulations of Drag and Separation Flow Around Ellipsoids, *Jordan Journal of Mechanical and Industrial Engineering*, 5, 2011, 129-132.
- [4]. Girma T. Bitsuamlaka, Agerneh K. Dagneb, James Erwinc, Evaluation of wind loads on solar panel modules using CFD, *The Fifth International Symposium on Computational Wind Engineering (CWE2010)*, 2010.
- [5]. Shaharin A Sulaiman, Chen Jiun Horng, Determinations of Drag and Lift using ANSYS CFD Flotran Simulation, 2006
- [6]. Georgeta Văsieș, Elena Axinte And Elena-Carmen Teleman, Numerical Simulation Of Wind Action On Solar Panel Placed On Flat Roofs With And Without Parapet, 2010.
- [7]. Bo Gong, Zhifeng Wang, Zhengnong Li, Jianhan Zhang, Xiangdong Fu, Field measurements of boundary layer wind characteristics and wind loads of a parabolic trough solar collector, *Solar Energy*, 86, 2012, 1880-1898.
- [8]. Jain A.K., *Fluid mechanics*, (Khanna Publishers, New Delhi, Tenth edition 2009).